JOURNAL GEOLOGICAL SOCIETY OF INDIA
Vol.85, April 2015, pp.500-508

Classification of Alteration Zones Based on Whole-rock Geochemical Data using Support Vector Machine

Maliheh Abbaszadeh[1], Ardeshir Hezarkhani[1] and Saeed Soltani-Mohammadi[2]
[1]Department of Mining and Metallurgy Engineering, Amirkabir University of Technology, Tehran, Iran.
[2]Department of Mining Engineering, University of Kashan, Kashan, Iran
Email: Abbaszadeh@aut.ac.ir; Abbaszadeh63@yahoo.com
ardeshir.hezarkhani@gmail.com; saeedsoltani@kashanu.ac.ir

Abstract: One of the most important steps in the mineral resource estimation and detailed exploration of porphyry copper deposit is separating the alteration zones as a control parameter of the copper grade. The most popular method for this separation is petrological investigations (other methods are not much popular), but the method lacks the ability to predict alteration zones of the un-sampled points. In this paper a new method has been proposed which is based on the support vector machine (SVM) classification of the analyzed whole rock samples and it has been used in Sungun porphyry copper deposit to separate potassic, phyllic and transition alteration zones. To apply the SVM method, use has been made of the radial basis function (RBF) as the kernel function and to obtain the optimal values for the SVM parameters (γ and C being the most important); the grid search method has been used. The best values for γ and C that have had good performance in the training and test steps are 0.0625 and 32, respectively. Results have revealed that the SVM classification (used in this study) can effectively separate the alteration zones in the Sungun deposit. Specifically, the accuracy of this method has been 75% which proves that the support vector machine can offer an inexpensive, fast and robust classification technique and it can be a valid alternative to the well established methodologies in this area.

Keywords: Porphyry Copper Deposit, Geochemical Data, Alteration, Support Vector Machine, Grid Search, Iran.

INTRODUCTION

Porphyry and porphyry related Cu–Mo deposits serve as the world's primary sources of Cu and Mo. They are formed by magmatic-hydrothermal fluids generated from subduction-related magmatism (Berger et al. 2008) and are mostly associated with oceanic and continental arc setting of Cenozoic age (Titley and Beane, 1981; Richards, 2003; Cooke et al., 2005 and Li et al., 2008). They are less commonly found in ancient fold belts (Titley and Beane, 1981).

Porphyry copper deposits (PCDs) are normally located beneath a comagmatic volcanic pile, which is transected by a column of hydrothermal alteration representing the upper parts of the porphyry copper system (Sillitoe, 1973). Hydrothermal alterations refer to metasomatic processes that change the composition, mineralogy, and texture of rocks that constitute a porphyry copper system (John et al., 2010).

Major hydrothermal alteration types commonly present in PCDs are (1) potassic, (2) phyllic (3) advanced argillic, (4) intermediate argillic, (5) propylitic, (6) sodic-calcic and sodic, (7) greisen, and (8) skarn (John et al., 2010), (Elliott et al., 1992).

Hydrothermal alteration mineral assemblages are zoned spatially and temporally and the zones have kilometer-scale vertical and lateral dimensions that show significant variation in geometry, largely as a function of rock composition, depth, and orientation of more permeable zones, such as hydro fractured rock and porphyry dikes. Most notably, potassic and phyllic alterations are invariably associated with sulfide mineralization in PCDs. They are generally zoned temporally, spatially, and thermally with respect to one another (John et al., 2010).

One of the most important steps in the mineral resource estimation and detailed exploration of porphyry copper deposit is separating the alteration zones as a control parameter of the Cu grade. The most popular method for this separation is petrological investigations , but the method lacks the ability to predict alteration zones of the un-sampled points (Asghari et al. 2008). In this paper a new method has been proposed which is based on the support vector classification of the analyzed whole rock samples.

STUDY AREA

Sungun PCD is in east Azarbaijan province, NW of Iran (Fig. 1). The magmatic suites in this area are part of the NW–SE trending Cenozoic magmatic belt of Iran and the porphyries occur as stocks and dikes (Calagari, 2003; Hezarkhani, 1997; Hezarkhani, 2002, 2003). This PCD is hosted in a diorite/granodioritic to quartz-monzonitic stock that intrudes Eocene volcanosedimentary and Cretaceous carbonate rocks (Hezarkhani, Williams-Jones, & Gammons, 1999). Three distinct types of hydrothermal alteration and mineralization are recognized at Sungun: (1) hypogene; (2) contact metasomatic and (3) supergene (Calagari, 2004).

Hypogene Hydrothermal Alteration and Mineralization

Four types of hypogene alterations have developed in the Sungun porphyry: (1) potassic; (2) potassic–phyllic (transition); (3) phyllic; and (4) propylitic (Calagari, 2003; Hezarkhani, 1997, 2002, 2003). The early hydrothermal alterations have been dominantly potassic and propylitic which were then followed by later transition and phyllic alteration (Hezarkhani and Williams-Jones, 1998). Hypogene mineralization occurs as disseminations, fracture and micro-fracture fillings. Contact metasomatic (e.g. skarns) alteration occurs in patches along the contact of Porphyry stock with upper Cretaceous carbonates. Two distinct supergene alteration zones are recognized at Sungun: (1) oxidized and leached, and (2) supergene sulfides (Calagari, 2004).

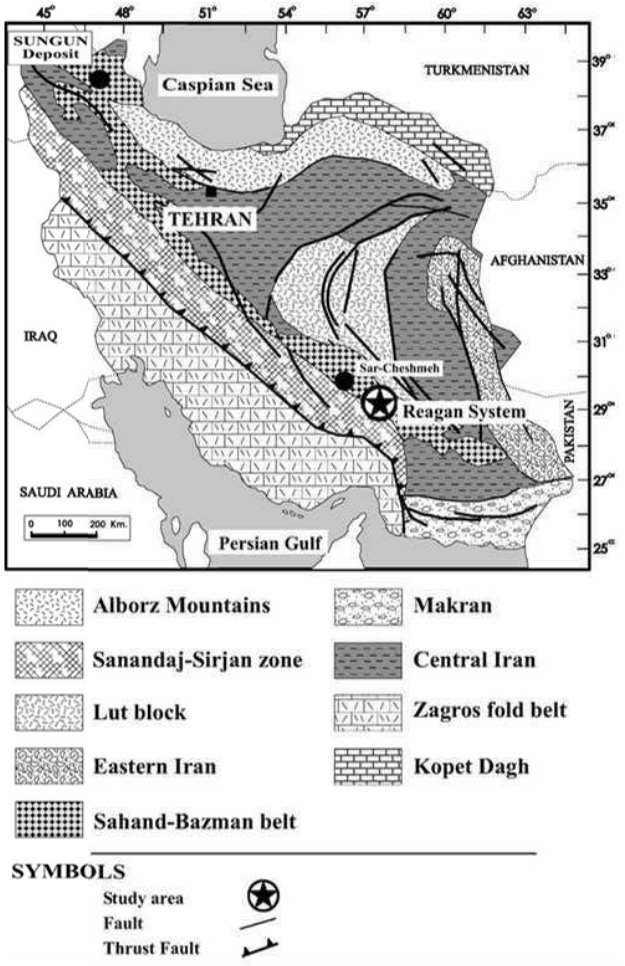

Fig.1. Geological map of Iran (modified from (Shahabpour, 1994)) showing major lithotectonic units.

Potassic Alteration

The earliest alteration is represented by potassic mineral assemblages developed pervasively and as halos around veins in the deep and central parts of the Sungun stock. Potassic alteration is characterized by K-feldspar. This alteration displays a close spatial association with mineralization. About 60% of the copper and all the molybdenum have been emplaced during this alteration episode (Hezarkhani and Williams-Jones, 1998) (Fig. 2).

Propylitic Alteration

There is a relatively sharp boundary between the Propylitic and potassic alteration zones in the deep part of the deposit, but at shallow levels this contact is obscured by the later phyllic alteration. Propylitic alteration is pervasive and is represented mainly by chloritization of the primary and secondary biotite, amphibole and groundmass material in the rocks peripheral to the central potassic zone (Hezarkhani and Williams-Jones, 1998) (Fig. 2).

Transition Alteration

Potassic alteration is overprinted by a large zone of pervasive transition alteration in the central part of the stock which grades upward into the phyllic alteration. Transition alteration is characterized by albite replacement of more An-rich plagioclase and albite rims around orthoclase. A distinguishing characteristic of this type of alteration is the white colour of the affected rocks (Hezarkhani and Williams-Jones, 1998) (Fig. 2).

Phyllic Alteration

The change from transition to phyllic alteration is gradual and is marked by an increase in the proportion of muscovite. Phyllic alteration is characterized by the replacement of almost all rock-forming silicates by sericite and quartz and overprints the earlier formed potassic and transition alterations (Hezarkhani and Williams-Jones, 1998) (Fig. 2).

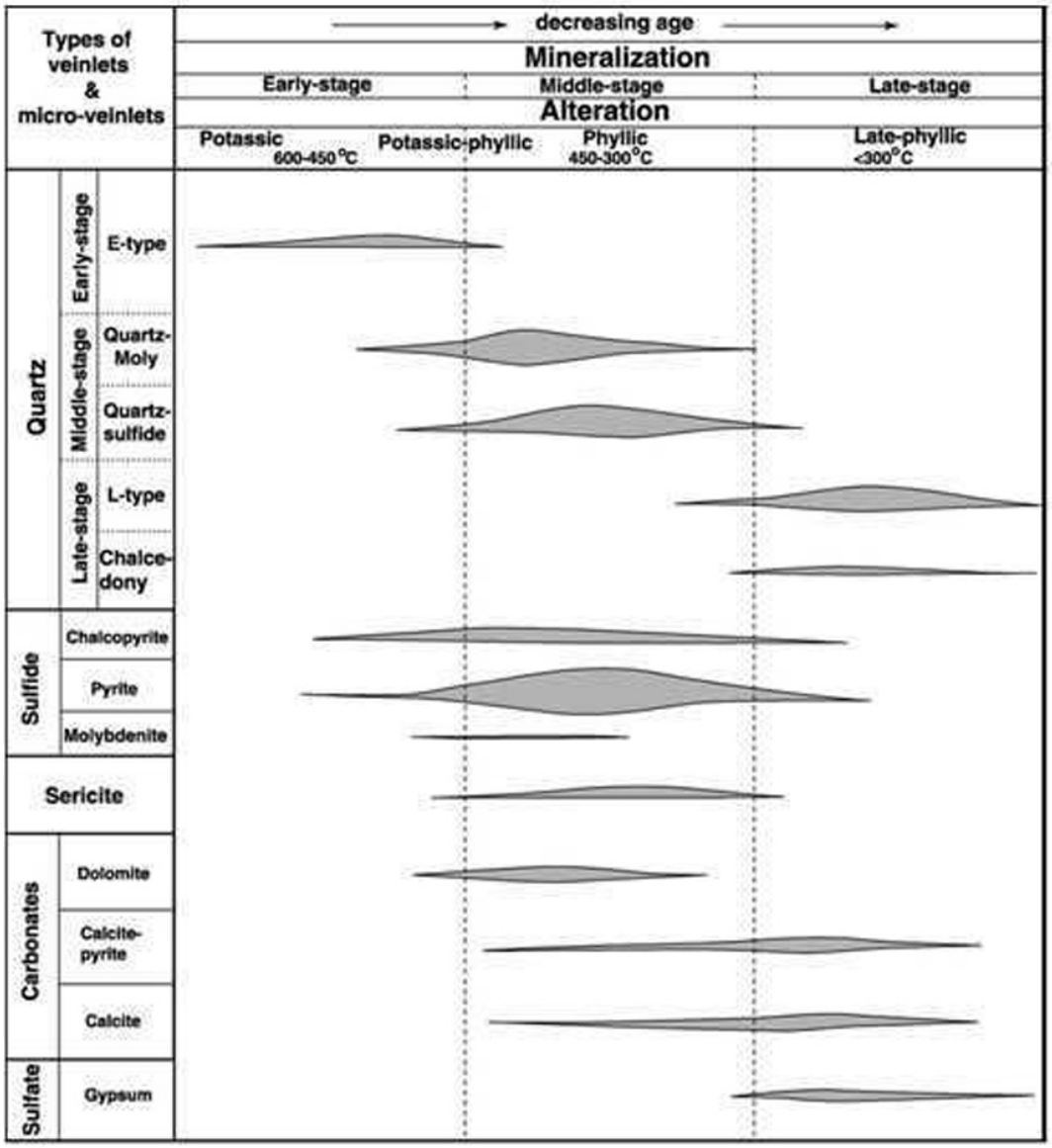

Fig.2. Paragenetic sequence of the development of various types of veinlets and micro-veinlets in porphyry stock II at Sungun. The thickness of the horizontal bars is related to the relative abundance of the veinlets (Hezarkhani andWilliams-Jones, 1998) and (Calagari, 2004).

Relationship between Mineralization and Alterations

Hypogene copper mineralization was formed during potassic alteration and to a lesser extent during phyllic alteration and exists as disseminations and in veinlet form. During potassic alteration, the copper mineralization consisted of chalcopyrite and minor bornite; later hypogene copper mineralization consisted mainly of chalcopyrite (Fig.2). Hypogene molybdenum mineralization (molybdenite) was concentrated mainly in the deep part of the stock and is associated exclusively with potassic alteration, where it is found in quartz veins accompanied by K-feldspar, anhydrite, sericite and lesser chalcopyrite. Copper mineralization increases toward the margins of the central potassic zone, from less than 0.20 to 0.85 wt.%. There is also a positive correlation between silicification and copper mineralization. The maximum Cu grade is associated with biotite, orthoclase and sericite (potassic zone) while the pyrite content is highest (3-10 vol. % of the rock) in the marginal quartz-sericite (phyllic) zone. The ratio of pyrite to chalcopyrite in the zone of the richest hypogene copper mineralization in the potassic alteration zone is as low as 4:1, but toward the margins of the stock the ratio increases to 15:1 (Hezarkhani and Williams-Jones, 1998).

DATA SET

Representative samples of altered diorite/granodiorite, monzonite/quartz monzonite, andesite and mineralized dykes were analyzed for major and trace element compositions. Detailed petrographic studies of wall rocks, veins and alteration zones were carried out on more than 100 hand samples and 60 polished thin sections. All samples were analyzed by XRF with a detection limit of 0.01 wt. % for major elements and 2 ppm for trace elements (except TiO_2 10 ppm, and Cu and Mo 1 ppm) (Hezarkhani, 2006). These whole-rock geochemical data were supplemented by the analyses from (Mehrpartou, 1993).

In this study, 78 whole-rock samples were analyzed for major and trace elements. The analyses included 10 major (e.g. SiO_2, TiO_2, Al_2O_3,…) and 18 trace (e.g. Ba, Ce, Co,…) elements of the representative altered rocks from the Sungun porphyry copper deposit. Since copper mineralization in Sungun is essentially associated more with potassic and less with phyllic and transition zones, these alterations have been made use of in this study. Descriptive statistics of 29, 28 and 21 samples respectively from potassic, phyllic and transition alteration zones, are presented in Table 1.

METHODOLOGY

Problem Statement

Let $S = \{x \mid x \in R^n\}$ be the set of all the possible whole-rock samples covering a deposit area. Each sample is represented by an *n*-dimensional real vector and every particular coordinate x_i represents the value of a measured property such as SiO_2, TiO_2, and Al_2O_3 which were analyzed by XRF. Let $C=\{c_1,c_2,...,c_l\}$ be the set of l classes that correspond to some such predefined alteration types as phyllic and potassic. The function $f_c:S\rightarrow C$ is called a classification if for each $x_i \in S$ it holds that $f_c(x_i)=c_j$ if x_i belongs to the class c_j. In practice, one has only a limited set of *m* labeled examples (x_i,y_i), $x_i \in R^n$, $y_i \in C$, $i=1,..., m$ and n is the number of properties used to describe each (whole-rock sample). Labeled examples form the training set for the classification. The machine learning approach tries to find the function $\hat{f}_c$, which is a good approximation of the real, unknown function f_c, using only the examples from the training set and a specific learning method such as support vector machine (Mitchell, 1997).

In this research, n= 28 (10 major and 18 trace elements) and m=3 (c_1: potassic, c_2: phyllic and c_3: transition).

Table 1. Descriptive statistics of whole- rock samples from Potassic, Phyllic and Transition alteration zones

Type	Potassic					Phyllic					Transition				
	Max	Min	Avg	Var	S.D.	Max	Min	Avg	Var	S.D.	Max	Min	Avg	Var	S.D.
SiO_2	70.7	54.9	62.4	13.5	3.7	72.4	57.3	68.4	14.0	3.7	71.1	59.7	64.0	9.6	3.1
TiO_2	1.0	0.4	0.6	0.0	0.1	0.8	0.2	0.5	0.0	0.1	0.6	0.2	0.5	0.0	0.1
Al_2O_3	18.8	14.1	15.8	0.9	0.9	16.3	13.0	15.1	1.0	1.0	16.7	14.3	15.5	0.3	0.5
Fe_2O_3	7.0	1.3	3.6	2.8	1.7	4.8	0.1	2.1	1.8	1.3	6.1	0.2	2.8	3.0	1.7
MnO	0.1	0.0	0.1	0.0	0.0	0.1	0.0	0.0	0.0	0.0	0.3	0.0	0.1	0.0	0.1
MgO	5.6	0.8	2.1	1.0	1.0	3.5	0.0	1.3	0.6	0.8	3.4	0.6	1.9	0.6	0.8
CaO	7.6	0.4	2.9	2.5	1.6	4.8	0.1	1.5	2.0	1.4	4.2	0.0	1.9	2.1	1.4
Na_2O	6.0	0.2	2.5	3.1	1.8	4.6	0.0	0.7	1.1	1.1	4.5	0.1	2.3	2.3	1.5
K_2O	6.9	1.7	4.5	2.6	1.6	5.2	0.2	4.4	0.9	1.0	7.4	2.4	4.7	1.5	1.2
P_2O_5	0.5	0.2	0.3	0.0	0.1	0.6	0.1	0.3	0.0	0.1	0.5	0.2	0.3	0.0	0.1
Ba	2044.0	20.4	1031.5	229146.34	78.7	1264.0	361.0	659.9	68570.8	261.9	1534.0	636.0	1088.2	72064.2	268..4
Ce	192.0	14.0	93.5	1901.6	43.6	215.0	0.0	71.1	2075.3	45.6	152.0	3.0	71.7	1056.9	32.5
Co	24.0	0.0	11.0	68.7	8.3	45.0	0.0	7.2	158.2	12.6	20.0	0.0	5.2	46.2	6.8
Cr_2O_3	269.0	40.0	82.6	3172.7	56.3	279.0	23.0	68.5	3919.2	62.6	132.0	36.0	76.7	1016.5	31.9
Cu	3050.0	36.0	3236.0	17212741.7	4148.8	16024.0	467.0	5526.3	24101396.8	4909.3	11856.0	43.0	2733.4	12126277.2	3482.3
Ni	96.0	15.0	38.8	589.7	24.3	154.0	0.0	42.4	1256.2	35.4	91.0	3.0	32.1	384.0	19.6
Sc	19.0	0.0	7.0	33.6	5.8	19.0	0.0	3.7	31.3	5.6	17.0	0.0	5.4	50.9	7.1
V	185.0	53.0	86.0	1169.5	34.2	106.0	17.0	69.2	461.0	21.5	95.0	48.0	67.8	153.0	12.4
Zn	2353.0	21.0	583.6	545481.67	38.6	1657.0	0.0	237.8	223474.6	472.7	64.0	0.0	31.1	597.9	24.5
Ga	19.0	0.0	12.5	47.8	6.9	39.0	0.0	14.0	65.0	8.1	2300.0	0.0	116.4	250404.5	500.4
Nb	22.0	9.0	15.5	12.0	3.5	23.0	1.0	14.3	24.2	4.9	19.0	6.0	14.1	9.0	3.0
Pb	36.0	0.0	16.6	69.6	8.3	22.0	0.0	5.1	50.1	7.1	50.0	0.0	9.5	247.6	15.7
Rb	124.8	34.0	88.5	720.0	26.8	125.0	61.0	91.0	191.5	13.8	137.0	57.0	99.1	287.4	17.0
Sr	1194.0	180.0	620.8	87735.8	296.2	1242.0	34.0	254.5	100145.1	316.5	1413.0	69.0	478.0	133390.4	365.2
Th	27.0	1.8	16.2	44.5	6.7	68.0	0.0	16.2	135.4	11.6	37.0	0.0	19.4	93.9	9.7
U	10.0	0.0	1.2	5.7	2.4	13.0	0.0	2.4	13.2	3.6	15.0	0.0	5.2	12.8	3.6
Y	18.0	7.0	12.8	9.7	3.1	15.0	1.0	7.6	19.8	4.5	17.0	2.0	10.2	13.4	3.7
Zr	169.0	104.8	124.8	351.0	18.7	169.0	88.7	136.3	359.7	19.0	152.0	64.0	124.8	440.2	21.0

1 - Maximum; 2 - Minimum; 3 - Variance; 4 - Standard Deviation

Support Vector Machine Classification

Classification is an important task in data mining which aims to predict the classes of future data objects. In classification, one builds a model (set of rules) from a group of classified training data objects in order to forecast the classes of previously unseen data objects. The data set used to learn the model is known as the training data set and the one used to measure the quality of the model is known as the testing data set (Thabtah and Cowling, 2007).

There are two types of classification techniques: supervised and unsupervised. A support vector machine (SVM) is a model of algorithms for the supervised type (Simin, et al., 2010; Zuo and Carranza, 2011). SVMs are theoretically well-justified machine learning techniques which have also been successfully applied to many real-world domains (Shawe-Taylor and Sun, 2011). Certain types of SVMs have been developed and applied successfully to text categorization, handwriting recognition and other studies (Yao et al., 2008; Zuo and Carranza, 2011). Nowadays, SVMs are being applied in some such geosciences and mining engineering problems as the remote sensing (Camps-Valls and Bruzzone, 2005; Camps-Valls et al., 2006; Camps-Valls and Bruzzone, 2009; Mountrakis et al., 2011; Petropoulos et al., 2012), mapping mineral prospectivity (Zuo and Carranza, 2011; Abedi et al., 2012), ore-rock classification (Seng and Chen, 2009), classification of the excavation damaged zones (Fattahi et al., 2013) and ore grade estimation (Perez et al., 2011).

SVMs try to find a linear separating hyperplane in the feature space (Taboadaet al. 2006; Salahshoor et al., 2010). Their key concept (originally developed for binary classification problems), is the use of hyperplanes to define decision boundaries separating training points of different classes (Luts et al., 2010). The training points that are closest to the optimal separating hyperplane are called support vectors. All other points are irrelevant to determining the binary class boundaries (Shin et al., 2005).

SVMs are able to handle both simple/linear and complex/nonlinear classification problems. The idea behind them is to map the original data points from the input space to a high-dimensional, or even infinite-dimensional, feature space so that the classification problem becomes simpler in the feature space (Luts et al., 2010) (Fig.3).

In the SVM method, the separating hyperplane can be defined in many ways, however, SVMs are based on the maximum margin principle and they aim at constructing a hyperplane with a maximal distance between the two classes (Fig.4) (Luts et al., 2010).

Classifying with the SVM is much more effective than

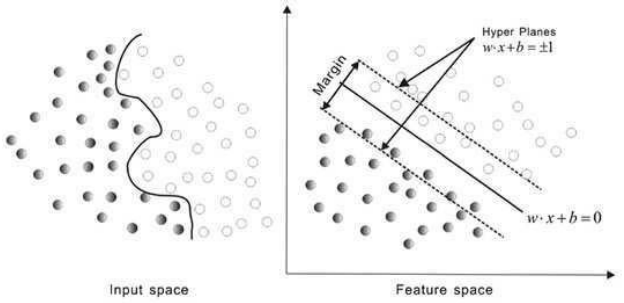

Fig.3. Support vectors and optimum hyperplane for the binary case of linearly separable data sets (Zuo and M.Carranza, 2011).

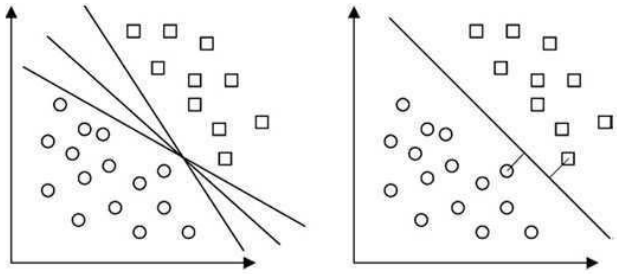

Fig.4. Left: Various hyperplanes allow separating the data. Right: SVMs construct a hyperplane that maximizes the margin (Luts et al., 2010).

with the other conventional non parametric classifiers (e.g., neural networks, nearest neighbors, maximum likelihood methods) in terms of classification accuracy and stability of parameter setting (Simin et al., 2010).

According to what was mentioned earlier, the classical task of an SVM is a binary (two-class) classification. Suppose we have a training set composed of l feature vectors $x_i \in R^n$, where i = 1, 2 … n is the number of the feature vectors in the training samples. The class to which each sample identified belong to is labeled y_i which is equal to 1 for one class or -1 for the other (i.e. $x_i \in \{-1, 1\}$). If the two classes are linearly separable, then there exists a family of linear separators, also called separating hyperplanes, which satisfy the following set of equations (Zuo and Carranza, 2011) (Fig.3).

$$wx_i + b \geq +1 \qquad \text{for } y_i = +1 \tag{1}$$

(w and b being the weight vector and bias value respectively)

which is equivalent to

$$y_i(wx_i + b) \geq 1 \qquad i = 1, 2, ..., n \tag{2}$$

The separating hyperplane can then be formalized as a decision function

$$f(x) = sgn\,(wx + b) \tag{3}$$

where, sgn is a sign function in the following form:

$$sgn(x) = \begin{cases} 1, & if\ x > 0 \\ 0, & if\ x = 0 \\ -1, & if\ x < 0 \end{cases} \quad (4)$$

The two parameters of the separating hyperplane decision function (w and b) can be obtained by solving the following optimization function:

$$\text{Minimize } \tau(w) = \tfrac{1}{2} \| w \|^2 \quad (5)$$

Subject to

$$y_i ((wx_i) + b) \geq 1, \qquad i = 1, ...,l \quad (6)$$

The solution to this optimization problem is the saddle point of the Lagrange function

$$L(w, b, \alpha) = \frac{1}{2} \| w \|^2 - \sum_{i=1}^{l} \alpha_i (y_i((x_i w) + b) - 1) \quad (7)$$

$$\frac{\partial}{\partial b} L(w, b, \alpha) = 0 \quad (8)$$

where α_i is a Lagrange multiplier. The Lagrange function is minimized with respect to *w* and *b* and is minimized with respect to $\alpha_i > 0$. Lagrange multipliers α_i are determined by the following optimization function:

Maximize

$$\sum_{i=1}^{l} \alpha_i - \frac{1}{2} \sum_{ij=1}^{l} \alpha_i \alpha_j y_i y_j (x_i x_j) \quad (9)$$

Subject to

$$\alpha_i \geq 0,\ i = 1,..., l, \quad \text{and } \sum_{i=1}^{l} \alpha_i y_i = 0 \quad (10)$$

The separating rule, based on the optimal hyperplane, is the following decision function (Zuo & M.Carranza, 2011):

$$f(x) = sgn\ (\Sigma_{i=1}^{l}\ y_i a_i (x x_i) + b) \quad (11)$$

In a linear SVM, a linear decision boundary is used to classify the training set. In case of non-separable data, the data set is not completely classified by the linear decision boundary. Non-separable points can be classified correctly by using a non-linear decision boundary. In general, models are not scalable from linear to non-linear regions, but SVMs can be converted from linear to non-linear modes with few changes. A non-linear SVM employs a non-linear decision function to classify the training set by mapping the non-separable data points to a higher dimension where they become separable. In the higher dimension, a linear decision boundary is located to classify the data set. This linear decision boundary becomes non-linear when mapped back into the input space. The data can be mapped to a higher Euclidean space H by a mapping function called φ (Ratnanjali and Satish, 2008):

$$\varphi : R^d \rightarrow H \quad (12)$$

As shown in equation (11), the input data comes in the dot product form. So, in a non-linear SVM, the decision function will depend on $\varphi(x_i).\ \varphi(x_j)$ instead of $x_i.x_j$. Therefore, the decision function becomes:

$$f(x) = sgn\ (\Sigma_{i=1}^{l}\ y_i \alpha_i (\varphi(x).\varphi(x_i)) + b) \quad (13)$$

Now, if there were a "kernel function" *K* such that

$$K(x_i, x_j) = \varphi(x_i).\ \varphi(x_j), \quad (14)$$

we would only need to use *K* in the training algorithm; we would never need to even know explicitly what φ is (Ratnanjali and Satish, 2008). Combining equations (11) and (14), the decision function can be rewritten as follows:

$$f(x) = sgn\ (\Sigma_{i=1}^{l}\ y_i \alpha_i K(x_i, x) + b) \quad (15)$$

The four popular kernel functions are as follows (Zuo and M.Carranza, 2011):

Linear: $K(x_i, x_j) = \lambda x_i x_j$

Polynomial of degree *d*:

$$K(x_i, x_j) = (\lambda x_i x_j + r)^d, > 0 \quad (16)$$

Radial basis function:

$$K(x_i, xK(x_i, x_j) = exp\ \{-\lambda \| x_i - x_j \|^2\}, \lambda > 0$$

Sigmoid:

$$K(x_i, x_j) = K(x_i, x_j) = \tanh(\lambda x_i x_j + r), \lambda > 0$$

where λ, *r* and *d* are referred to as the kernel parameters; λ serves as an inner product coefficient in the polynomial function. In the case of the Radial Basis Function (RBF) kernel (EQ. (16)), λ determines the RBF width. In the sigmoid kernel, λ serves as an inner product coefficient in the hyperbolic tangent function. Parameter *r* is used for the kernels of the polynomial and sigmoid types; it is the degree of a polynomial function (Zuo and Carranza, 2011).

In our study, RBF kernel has been used because it can analyze higher-dimensional data and requires that only two parameters C (penalty parameter) and λ be defined. Therefore, to design an SVM, one must choose a kernel function, set the kernel parameters, and determine a soft margin constant C (Huang and Wang, 2006).

Originally, support vector machines were designed for binary classification. Currently there are several methods that have been proposed for such multi-class classifications as one-against-one, one-against-all, and directed acyclic graph (DAG); (Hsu and Lin, 2002; Milgram et al., 2006) have compared these methods. Generally, for problems with

few classes, like our problem, the "one against all" strategy seems significantly more accurate; while for problems with a very large number of classes, the "one against one" strategy is more suitable. In this study, the "one against all" method has been used to separate different alteration zones, by taking one class as +1 and other classes as -1.

MODELING FRAMEWORK

The modeling framework for using the SVM consists of the following steps:

1. Preparation of the training and testing data sets.
2. Training the model (using the training data set).
3. Cross-validating the model (using the training data sets/subsets).
4. Testing the trained model (using the testing data set).

Step 1 involves the development of the training and testing data sets. It is important to prepare these sets with similar statistical characteristics some of which are the maximum and minimum values, size of the data sets, average, variance, standard deviation and the range. Data sets for the tests were extracted (at regular intervals) from the sorted database, and the remaining data sets were used for the training. In the present study, 62 data sets (approximately 80%) were used for the training and the remaining 16 (approximately 20%) were chosen to test the model. In step 2, the model is trained to estimate the optimal parameter using the training data set. Then, the model is cross-validated using the training data sets/sub-sets in step 3. The training data sub-set is prepared following the procedure described in step 1. Different such sub-sets may be used to cross validate the model to ensure the stability of the mode parameter estimates. In step 4, the model is tested using the testing data set; this step is vital to ensure that the model has not seen the testing data set before.

RESULTS AND DISCUSSION

According to the modeling framework and the methodology described above, the training and testing data sets were created from the original database. The tests data sets were extracted at regular intervals from the sorted database, and the remaining sets were used for training. In the present study, 62 data sets (approximately 80%) were used for the training, and the remaining 16 sets (approximately 20%) were chosen to test the model.

In this paper, the LIBSVM function (Chang and Lin, 2011) in the Weka software (Hall et al., 2009) has been used for the SVM classification. We have used the RBF kernel because it can analyze higher-dimensional data and requires that only C and γ be defined. These parameters were estimated through a grid search approach (Hsu et al., 2010) for the SVM model. In this approach, various (C, γ) pair values are tried and the one with the best cross-validation accuracy is picked. In the present paper, we made use of the exponentially growing sequences of C and γ, according to (Hsu et al., 2010), as a practical method to identify good parameters (for example, C= 2^{-5}, 2^{-3}, …, 2^{15} and $\gamma = 2^{-15}$, 2^{-13},…, 2^{3}).

Since a complete grid search could still be time-consuming, we first made a coarse one and then used C= 2^{-5}, 2^{-3}, …, 2^{15} and $\gamma = 2^{-15}$, 2^{-13},…, 2^{3} ranges. It is worth mentioning that after identifying a "better" region on the grid, a finer grid search can be conducted on that region (C= 2^{-1}, 2^{0},…, 2^{5} and γ= 2^{-6}, 2^{-5},…, 2^{0}). Therefore, in this paper, to build the SVM model for the classification and separation of potassic, phyllic and transition alteration zones, after scaling the training set and using a coarse grid (Fig.5), we first found that the best (C, γ) was (2^{2}, 2^{-3}) with a cross-validation rate of 62.9%. Next, we conducted a finer grid search on the neighborhood of (2^{2}, 2^{-3}) (Fig.6) and obtained a better cross-validation rate of 69.35% at (2^{5}, 2^{-4}). After the best (C, γ) was found, the entire training set was trained again to generate the final classifier. To achieve this goal, we made use of the grid search method and the LIBSVM function in the Weka software (version 3.6).

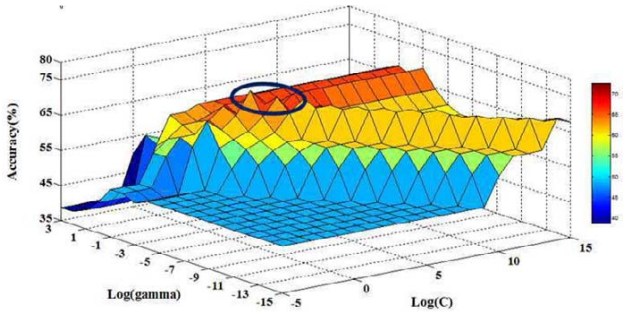

Fig.5. Three-dimensional surface plot of the coarse grid search against percentage of model accuracy. C and ã are parameters the SVM method.

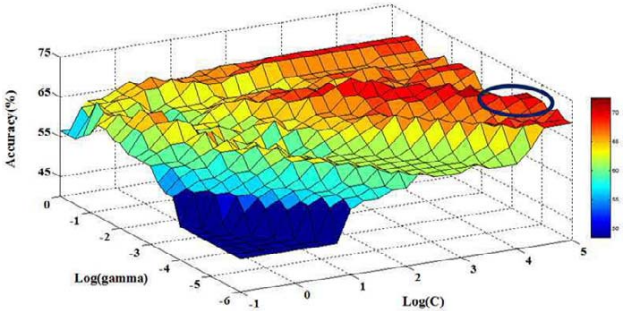

Fig.6. Three-dimensional surface plot of the fine grid search against percentage of model accuracy. C and ã are parameters the SVM method.

Table 2. SVM model parameters for training and testing data

Parameter	Value
SVM type	C-SVM
Kernel function	RBF
γ	0.0625
C (Penalty Parameter)	32

Table 3. Confusion matrix for training data (RBF kernel)

LIBSVM				
True		Potassic	Transition	Phyllic
Classified as				
	Potassic	20	2	1
	Transition	1	16	0
	Phyllic	0	0	22

Table 4. Confusion matrix for testing data (RBF kernel)

LIBSVM				
True		Potassic	Transition	Phyllic
Classified as				
	Potassic	4	0	1
	Transition	1	1	2
	Phyllic	0	0	7

Using the LIBSVM function on the whole training data set (62 samples) and the (2^5, 2^{-4}) set as the best values for C and γ respectively, we obtained the accuracy of about 93.55% for the training data. By implementing the LIBSVM model on the test data (16 samples) and setting (2^5, 2^{-4}) as the best values for C and γ respectively, the accuracy obtained was 75%. The best SVM parameters for the training and test data are presented in Table 2 and the related confusion matrices are shown in Tables 3 and 4, respectively.

CONCLUSIONS

In this study, the SVM was used to separate the potassic, phyllic and transition alteration zones in Sungun PCD and the SVM model proved to have good capability to classify and separate the alteration zones using geochemical data. According to this study, it is established that the SVM approach seems to be a good option for the accurate separation and classification of potassic, phyllic and transition alteration zones. Results indicate that if model parameters such as γ and C are selected properly, the SVM algorithm can classify and separate the alteration zones satisfactorily. It was found that by selecting 0.0625 as an optimum value for γ it guarantees the separation of potassic, phyllic and transition alteration zones in the training and test data with the accuracy of about 93.55% and 75% respectively. This model is very fast and helps to avoid wasting of time and money. Besides, by saving time and money, we can focus on the target exploration area in our next investigations and drilling operations. In addition, this method can be very useful for geochemists in separating the alteration zones, because classifying and separating samples microscopically is quite time consuming. According to the obtained results, the support vector machine can be a powerful tool for mining problems, and mining engineers and geologist can achieve better and more reliable results in most of the earth science classification.

References

Abedi, M., Norouzi, G.H. and Bahroudi, A. (2012) Support vector machine for multi-classification of mineral prospectivity areas. Computers & Geosciences, v.46, pp.272-283.

Asghari, O., Hezarkhani, A. and Rafiee, V. (2008) Applying discriminat amalysis and SGS to separating alteration zones within the Sungun porphyry copper deposit. Paper presented at the 8th International Scientific Conference - SGEM2008.

Berger, B.R., Ayuso, R.A., Wynn, J.C. and Seal, R.R. (2008). Preliminary model of porphyry copper deposits: U.S. Geological Survey Open-File Report 2008–1321, 55p.

Calagari, A. A. (2003) Stable isotope (S, O, H and C) studies of the phyllic and potassic–phyllic alteration zones of the porphyry copper deposit at Sungun, East Azarbaidjan, Iran. Jour. Asian Earth Sci., v.21, pp.767–780.

Calagari, A. A. (2004). Fluid inclusion studies in quartz veinlets in the porphyry copper deposit at Sungun, East-Azarbaidjan, Iran. Jour. Asian Earth Sci., v.23, pp.179-189.

Camps-Valls, G. and Bruzzone, L. (2005) Kernel-based methods for hyperspectral image classification. IEEE Transactions on Geoscience and Remote Sensing, v.43(6), pp.1351–1 362.

Camps-Valls, G. and Bruzzone, L. (2009) Kernel methods for Remote Sensing Data Analysis. Wiley & Sons, UK.

Camps-Valls, G., Gómez-Chova, L., Muñoz-Marí, J., Vila-Francés, J. and Calpe-Maravilla, J. (2006) Composite kernels for hyperspectral image classification. IEEE Geoscience and Remote Sensing Lett., v.3(1), pp.93-97.

Chang, C.C. and Lin, C.J. (2011) LIBSVM: a library for support vector machines. ACM Trans. Intelligent Systems and Technology, v.2, pp.27:1–27:27.

Cooke, D., Hollings, P. and Walsh, J. (2005). Giant porphyry deposits: characteristics, distribution, and tectonic controls. Econ. Geol., v.100, pp.801–818.

Elliott, J.E., Wallace, C.A., Lee, G.K., Antweiler, J.C., Lidke, D.J., Rowan, L.C., et al. (1992) Maps showing mineral resource assessment for skarn deposits of gold, silver, copper, tungsten, and iron in the Butte 1° x 2° Quadrangle, Montana: USGS Misc Investigations Series, I-2050-E.

Fattahi, H., Ebrahimi Farsangi, M. A., Shojaee, S., Nekooei, K. and Mansouri, H. (2013) Application of the Hybrid Harmony Search with Support Vector Machine for Identification and Classification of Damaged Zone around Underground Spaces. Internat. Jour. Optimization in Civil Engg., v.3(2), pp.345-358.

Hall, M., Frank, E., Holmes, G., Pfahringer, B., Reutemann, P. and Witten, I.H. (2009) The WEKA Data Mining Software:

An Update; SIGKDD Explorations, Volume 11, Issue 1.

Hezarkhani, A. (1997) Physicochemical controls on alteration and copper mineralization in the Sungun porphyry copper system, Iran. University of McGill, Montreal, Quebec, Canada.

Hezarkhani, A. (2002) Specific Physico-Chemical Conditions (360 °C) for Chalcopyrite Dissolution/Porphyry system in the Reagan Porphyry Copper Porphyry system, Iran. Amirkabir Jour. Sci. Tech., v.13(52), pp.668–687.

Hezarkhani, A. (2003) Hydrothermal evolution in the Raigan porphyry copper system based on fluid inclusion studies, (Kerman, Iran): the path to an uneconomic deposit. Amirkabir Jour. Sci. Tech., v.15, pp.74–84.

Hezarkhani, A. (2006) Petrology of the intrusive rocks within the Sungun Porphyry Copper Deposit, Azerbaijan, Iran. Jour. Asian Earth Sci., v.27, pp.326–340.

Hezarkhani, A. and Williams-Jones, A.E. (1998) Controls of alteration and mineralization in the Sungun Porphyry Copper Deposit, Iran: evidence from fluid inclusions and stable isotopes. Econ. Geol., v.93, pp.651–670.

Hezarkhani, A., Williams-Jones, A.E. and Gammons, C.H. (1999) Factors controlling copper solubility and chalcopyrite dissolution in the Sungun porphyry copper deposit, Iran. Mineralium Deposita, v.34, pp.770–783.

Hsu, C.W., Chang, C.C. and Lin, C.J. (2010) A Practical Guide to Support Vector Classification, Technical Report (pp.1-12): Department of Computer Science and Information Engineering, University of National Taiwan, Taipei.

Hsu, C.W. and Lin, C.J. (2002) A comparison of methods for multiclass support vector machines. IEEE Trans. Neural Networks, v.13(2), pp.415-425.

Huang, C.-L. and Wang, C.-J. (2006) A GA-based feature selection and parameters optimization for support vector machines. Expert Systems with Applications, v.31, pp.231–240.

John, D. A., Ayuso, R. A., Barton, M. D., Blakely, R. J., Bodnar, R. J., Dilles, J. H., et al. (2010) Porphyry copper deposit model, chap. B of Mineral deposit models for resource assessment: USGS Scientific Investigations Report 2010–5070–B. 169.

Li, J.-W., Zhao, X.-F., Zhou, M.-F., Vasconcelos, P., Ma, C.-Q., Deng, X.-D., et al. (2008) Origin of the Tongshankou porphyry–skarn Cu–Mo deposit, eastern Yangtze craton, Eastern China: geochronological, geochemical, and Sr–Nd–Hf isotopic constraints. Mineralium Deposita, v.43(3), pp.315-336.

Luts, J., Ojeda, F., Plas, R. V. d., Moor, B. D., Huffel, S. V. and Suykens, J. A. K. (2010) A tutorial on support vector machine-based methods for classification problems in chemometrics. Analytica Chimica Acta, v.665, pp.129–145.

Mehrpartou, M. (1993) Contributions to the geology, geochemistry, ore genesis and fluid inclusion investigations on Sungun Cu-Mo porphyry deposit, (Northwest of Iran).

Milgram, J., Cheriet, M. and Sabourin, R. (2006) One Against One" or "One Against All": Which One is Better for Handwriting Recognition with SVMs?" 10th Internat. Workshop on Frontiers in Handwriting Recognition, pp. 10-23.

Mitchell, T.M. (1997) Machine Learning. McGraw Hill, New York, 414p.

Mountrakis, G., Im, J. and Ogole, C. (2011) Support vector machines in remote sensing: A review. ISPRS Jour. Photogrammetry and Remote Sensing, v.66(3), pp.247-259.

Perez, C. A., Estevez, P. A., Vera, P. A., Castillo, L. E., Aravena, C. M., Schulz, D. A., et al. (2011) Ore grade estimation by feature selection and voting using boundary detection in digital image analysis. Internat. Jour. Mineral Processing, v.101, pp.28-36.

Petropoulos, G.P., Kalaitzidis, C. and Vadrevu, K.P. (2012) Support vector machines and object-based classification for obtaining land-use/cover cartography from Hyperion hyperspectral imagery. Computers & Geosci., v.41, pp.99-107.

Ratnanjali, S. and Satish, K. (2008) The Effect of Kernal Function on Classification. Paper presented at the XXXII National Systems Confernece, NSC-2008, December, 17-19.

Richards, J. P. (2003) Tectono-Magmatic Precursors for Porphyry Cu-(Mo-Au) Deposit Formation. Econ. Geol., v.98, pp.1515-1533.

Salahshoor, K., Kordestani, M. and Khoshro, M.S. (2010). Fault detection and diagnosis of an industrial steam turbine using fusion of SVM (support vector machine) and ANFIS (adaptive neuro-fuzzy inference system) classifiers. Energy, v.35, pp.5472-5482.

Seng, D. and Chen, W. (2009). Application of RS Theory and SVM in the Ore-Rock Classification. Paper presented at the Computational Intelligence and Software Engineering, 2009. CiSE 2009. International Conference on.

Shahabpour, J. (1994). Post-mineralization breccia dike from the Sar-Cheshmeh porphyry copper deposit, Kerman, Iran. Explor. Mining Geol., v.3, pp.39–43.

Shawe-Taylor, J. and Sun, S. (2011) A review of optimization methodologies in support vector machines. *Neurocomputing, 74*, 3609–3618.

Shin, K.-S., Lee, T.S. and Kim, H.-j. (2005) An application of support vector machines in bankruptcy prediction model. Expert Systems with Applications, v.28, pp.127–135.

Sillitoe, R. H. (1973) The Tops and Bottoms of Porphyry Copper Deposits. Econ. Geol., v.68, pp.799-815.

Simin, C., Rongqun, Z., Liming, L. and De, Z. (2010) A method of salt-affected soil information extraction based on a support vector machine with texture features. Mathematical and Computer Modelling, v.51, pp.1319-1325.

Taboada, J., Matías, J. M., Araújo, M. and Ordóñez, C. (2006) Assessing the viability of underground slate mining by combining an expert system with a GIS. Engg. Geol., v.87, pp.75–84.

Thabtah, F.A. and Cowling, P.I. (2007) A greedy classification algorithm based on association rule. Applied Soft Computing, v.7, pp.1102–1111.

Titley, S. and Beane, R. (1981) Porphyry copper deposits. Part 1. Geologic settings, petrology, and tectogenesis. Econ. Geol., v.75, pp.214–235.

Yao, X., Tham, L.G. and Dai, F.C. (2008) Landslide susceptibility mapping based on Support Vector Machine: A case study on natural slopes of Hong Kong, China. Geomorphology, v.101, pp.572–582.

Zuo, R. and M.Carranza, E. J. (2011) Support vector machine: A tool for mapping mineral prospectivity. Computers & Geosciences, v.37, pp.1967–1975.

(Received: 17 July 2013; Revised form accepted: 23 September 2013)